The concentration-pressure phase diagram for Zr-rich $PbZr_{1-x}Ti_xO_3$ ceramics

2000 J. Phys.: Condens. Matter 12 7295

(http://iopscience.iop.org/0953-8984/12/32/313)

J. Phys.: Condens. Matter **12** (2000) 7295–7302. Printed in the UK PII: S0953-8984(00)14278-X

The concentration–pressure phase diagram for Zr-rich $PbZr_{1-x}Ti_xO_3$ ceramics

A G Souza Filho†§, P T C Freire†, A P Ayala†, J M Sasaki†, I Guedes†, J Mendes Filho†, F E A Melo†, E B Araújo‡ and J A Eiras‡

† Departamento de Física, Universidade Federal do Ceará, Caixa Postal 6030, 60455-760 Fortaleza, Ceará, Brazil

‡ Departamento de Física, Universidade Federal de São Carlos, Caixa Postal 676, 13565-670 São Carlos, São Paulo, Brazil

E-mail: agsf@fisica.ufc.br (A G Souza Filho)

Received 25 May 2000, in final form 5 July 2000

Abstract. This work reports on systematic high-pressure Raman studies of the $PbZr_{1-x}Ti_xO_3$ ($0.02 \leqslant x \leqslant 0.14$) ceramics performed at room temperature. The pressure dependence of the Raman spectra reveals the stable phases of the material under pressure variation. The results allowed us to propose a concentration–pressure phase diagram for the Zr-rich PZT system up to pressures of 5.0 GPa.

1. Introduction

Lead zirconate titanates, $PbZr_{1-x}Ti_xO_3$, are widely known for their technological importance in the fields of electronics, sensors, and non-volatile ferroelectric memory devices. Due to this, PZT in different forms (ceramics, single crystals, and thin films) has been one of the most studied ferroelectric materials for over 50 years. It has been investigated by several experimental techniques such as x-ray and neutron diffraction [1–4], electric measurements [5, 6], and Raman spectroscopy [7–14]. This system presents an interesting concentration–temperature (x–T) phase diagram and its physical properties can be associated with several structural modifications [14]. Depending on the x-value, PZT exhibits at ambient pressure and room temperature different phases as follows [15]. For $0 \leqslant x \leqslant 0.05$, PZT presents an orthorhombic antiferroelectric structure belonging to the C_{2v}^8 space group. For x varying from 0.05 to 0.37, PZT presents a rhombohedral ferroelectric low-temperature phase F_R(LT) belonging to the space group C_{3v}^5, and from 0.37 to 0.48 presents a rhombohedral ferroelectric high-temperature phase F_R(HT) belonging to the space group C_{3v}^6. The composition around $x = 0.48$ defines a region known as the morphotropic phase boundary (MPB) which divides the rhombohedral from the tetragonal phases. From $x = 0.48$ to $x = 1.0$, PZT exhibits a tetragonal structure belonging to the space group C_{4v}^1. Recently, new features of the MPB region were reported [16, 17]. A new monoclinic ferroelectric phase belonging to the C_s^2 space group was discovered at low temperatures and studies on this new phase by techniques including high-resolution synchrotron x-ray powder diffraction, dielectric measurements [16, 17], and Raman spectroscopy [18] were reported.

§ Author to whom any correspondence should be addressed. Telephone: +55 85 2889912.

0953-8984/00/327295+08$30.00

There have been several theoretical and experimental efforts made to determine the thermodynamically stable phase of PZT when the pressure varies. Cerdeira *et al* [19] have studied the behaviour of $PbTiO_3$ single crystals up to 8.0 GPa. The pressure dependence of the lowest E(TO) soft-mode frequency obeys the Curie–Weiss law which predicts that $PbTiO_3$ undergoes a structural phase transition from a ferroelectric tetragonal to a cubic paraelectric phase at a pressure of about 9.0 GPa. Bäuerle *et al* [20] have studied $PbZr_{0.90}Ti_{0.10}O_3$ ceramics by using Raman spectroscopy with pressures up to 6.85 GPa. They showed that the material undergoes a phase transition at 0.57 GPa from the initial room temperature–ambient-pressure $F_R(LT)$ phase to a high-temperature rhombohedral phase. Between 0.8 and 0.91 GPa, $PbZr_{0.90}Ti_{0.10}O_3$ goes to the orthorhombic antiferroelectric phase, and between 3.97 and 4.2 GPa, a new phase is reached, with a symmetry higher than that of the antiferroelectric phase.

Recently, by means of dielectric, x-ray, and Raman measurements, Kobayashi *et al* [21] and Furuta *et al* [22] showed that a $PbZrO_3$ polycrystalline fine-powder sample undergoes a rich phase transition sequence up to 30 GPa: from the antiferroelectric phase to an orthorhombic phase I′ at 2.3 GPa, from an orthorhombic phase I′ to an orthorhombic phase I″ at 17.5 GPa, and finally from an orthorhombic phase I″ to a monoclinic phase at 23 GPa. More recently, Souza Filho *et al* [23] have studied $PbZr_{0.94}Ti_{0.06}O_3$, which besides presenting at room temperature the same phase as $PbZr_{0.90}Ti_{0.10}O_3$ [20], presents a sequence of phase transitions very different from those undergone by the latter. This indicates the richness of the PZT concentration–pressure phase diagram.

The purpose of this work is to investigate the structural properties of $PbZr_{1-x}Ti_xO_3$ ceramics under high hydrostatic pressure through micro-Raman spectroscopy. A careful analysis of the Raman spectra of samples with six different x-values yielded information concerning the different stable phases of $PbZr_{1-x}Ti_xO_3$ under pressure variation. On the basis of previous Raman and x-ray investigations of $PbZr_{1-x}Ti_xO_3$ and $PbZrO_3$, we propose a concentration–pressure phase diagram for Zr-rich PZT systems up to pressures of 5.0 GPa for $0.02 \leqslant x \leqslant 0.14$.

2. Experimental procedure

The preparation of our samples is described elsewhere [23]. Raman microprobe spectroscopy experiments were performed at room temperature in the backscattering geometry using the 514.5 nm radiation line of an Ar-ion laser for excitation. The backscattered light was analysed by using a Jobin-Yvon Triplemate 64000. A N_2-cooled charge-coupled-device (CCD) detector was used to detect the Raman signal. The spectrometer slits were set for a 2 cm^{-1} spectral resolution. An Olympus microscope lens and an objective with a numerical aperture NA = 0.80 were employed to focus the laser beam on the polished sample surface. The laser power impinging on the sample surface was of the order of 1.0 mW. The pressure cell was a diamond anvil cell (DAC) with 4:1 methanol:ethanol as the transmitting fluid. The pressure values were achieved with the well known pressure shift of the ruby luminescence lines [24]. In view of the laser heating the sample, the temperature in the laser spot was estimated, by means of the Stokes/anti-Stokes ratio. The temperatures obtained thus were close to room temperature (25 °C), with an error of about ±5 °C.

3. Results and discussion

3.1. The orthorhombic antiferroelectric phase—$PbZr_{1-x}Ti_xO_3$ with $0.02 \leqslant x \leqslant 0.04$

Figure 1 shows the unpolarized Raman spectra for $PbZr_{0.98}Ti_{0.02}O_3$. At room temperature and ambient pressure, this composition has an orthorhombic structure belonging to the space group

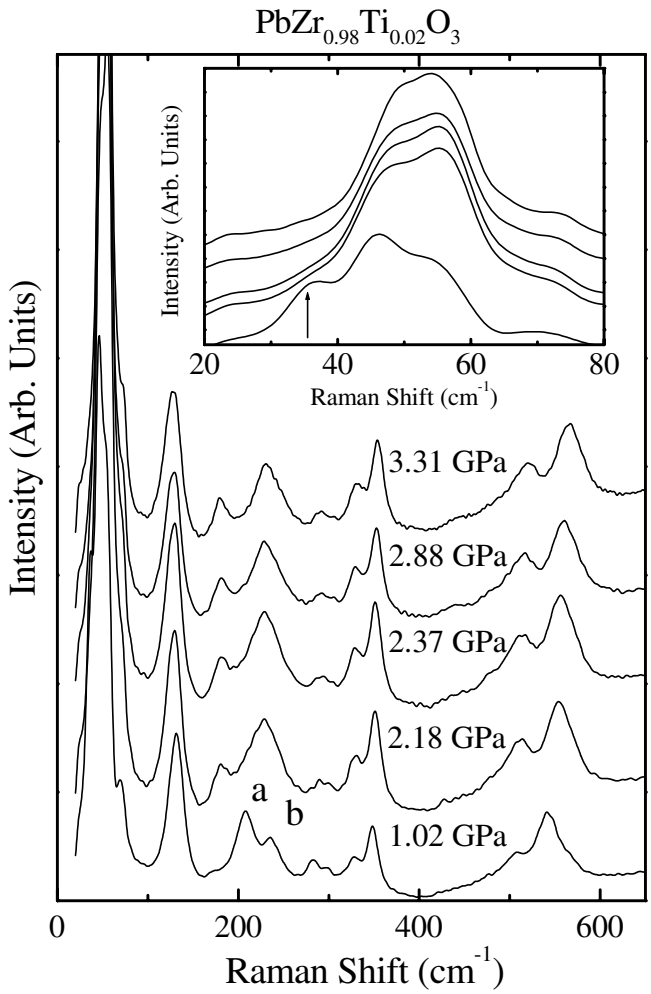

Figure 1. Raman spectra for $PbZr_{0.98}Ti_{0.02}O_3$ ceramics recorded at pressures up to 5.0 GPa. The inset depicts the external region mode.

C_{2v}^8 like $PbZrO_3$ [25]. Below 80 cm^{-1} (the spectral region depicted in the inset of figure 1), five modes at frequencies of 35, 44, 50, 55, and 70 cm^{-1} are observed. This spectral region contains the external modes related to Pb-lattice modes [26]. In the high-frequency region, $150 \leqslant \omega \leqslant 1000$ cm^{-1}, some internal modes related to certain polyatomic groups of the material appear in the Raman spectra. The assignment of these bands can be summarized as follows:

(i) the bands at 204, 232 cm^{-1} are associated with Zr–O bending;
(ii) the bands at 285, 330, and 344 cm^{-1} are assigned to ZrO_3 torsion; and
(iii) those at 501 and 532 cm^{-1} are due to the Zr–O stretching.

The assignments of these bands are based on work with $PbZrO_3$ single crystals [25].

To understand the pressure dependence of the Raman spectra for $PbZr_{0.98}Ti_{0.02}O_3$, let us recall the main results obtained by Furuta *et al* [22] on polycrystalline $PbZrO_3$ up to a pressure of 5.0 GPa. These authors showed that the left-hand-side mode of the doublet located at

about 210 cm^{-1} disappears at pressures higher than 2.3 GPa and that the right-hand-side mode increases in intensity. This spectral change is attributed to the orthorhombic (I) antiferroelectric phase → orthorhombic (I′) phase transition already determined by means of high-pressure x-ray diffraction measurements. For $PbZr_{0.98}Ti_{0.02}O_3$ the doublet mode is characterized by bands at 207 (labelled with **a** in figure 1) and 232 cm^{-1} (labelled with **b** in figure 1). Upon increasing pressure, the spectral features for the doublet are the same as those found in $PbZrO_3$. This spectral change observed for $PbZr_{0.98}Ti_{0.02}O_3$ around 2.18 GPa indicates the orthorhombic (I) antiferroelectric phase → orthorhombic (I′) phase transition. Moreover, the transition can be clearly identified by drastic changes in the lattice mode region (see the inset in figure 1), in particular through the observation of a band (marked with an arrow) that is not present in the spectra of the high-pressure phase.

For pressures above 2.18 GPa and up to 4.0 GPa, the Raman spectra remain the same, suggesting that the material did not undergo additional structural phase transitions like $PbZrO_3$ [21, 22]. The Raman spectra of $PbZr_{0.96}Ti_{0.04}O_3$ are qualitatively similar to those of $PbZr_{0.98}Ti_{0.02}O_3$. The only difference is that the pressure where the phase transition from the orthorhombic phase (I) to the orthorhombic phase (I′) occurs is 2.4 for $PbZr_{0.96}Ti_{0.04}O_3$.

3.2. The rhombohedral ferroelectric phase—$PbZr_{1-x}Ti_xO_3$ with $0.10 \leqslant x \leqslant 0.14$

This set of samples presents at room temperature and ambient pressure a rhombohedral structure belonging to the C_{3v}^6 space group [15]. First, let us describe the pressure dependence of the Raman spectra for $PbZr_{0.94}Ti_{0.06}O_3$ and $PbZr_{0.92}Ti_{0.08}O_3$. The former was the subject of our recent work [23] where we showed that $PbZr_{0.94}Ti_{0.06}O_3$ undergoes two different phase transitions up to 3.7 GPa as follows:

$$\text{rhombohedral (LT)} \overset{0.3\ \text{GPa}}{\rightarrow} \text{orthorhombic (I)} \overset{2.9\ \text{GPa}}{\rightarrow} \text{orthorhombic (I}').$$

These phase transitions and the pressure dependence of the Raman-active modes were described in detail elsewhere [23]. It should be pointed out that the composition $PbZr_{0.92}Ti_{0.08}O_3$ has exactly the same pressure dependence and the transitions

$$\text{rhombohedral (LT)} \rightarrow \text{orthorhombic (I)} \rightarrow \text{orthorhombic (I}')$$

occur at 0.5 and 3.4 GPa, respectively.

Figure 2 shows the Raman spectra for $PbZr_{0.90}Ti_{0.10}O_3$ recorded at different pressures. Bäuerle *et al* [20] have reported for the $PbZr_{0.90}Ti_{0.10}O_3$ composition the following sequence of pressure-induced phase transitions:

$$\text{rhombohedral (LT)} \overset{0.57\ \text{GPa}}{\rightarrow} \text{rhombohedral (HT)} \overset{0.8\ \text{GPa}}{\rightarrow} \text{orthorhombic (I)} \overset{3.9\ \text{GPa}}{\rightarrow} \text{higher-symmetry phase (probably cubic).}$$

Our results agree in part with those reported in reference [20]: in the pressure range of 0.0–1.0 GPa, we found the same sequence of phase transitions. Unfortunately, Bäuerle *et al* [20] did not report on the spectral region above 200 cm^{-1}. Observing the double bands (labelled with **a** and **b**) of the spectra in the inset of figure 2, it is clear that the stable phase above 4.2 GPa for $PbZr_{0.90}Ti_{0.10}O_3$ is the orthorhombic phase I′ [21, 22]. Thus, the transition observed in $PbZr_{0.90}Ti_{0.10}O_3$ [20] at 3.9 GPa is from an antiferroelectric orthorhombic phase to the orthorhombic I′ phase instead of from an antiferroelectric orthorhombic to a paraelectric cubic phase as proposed by Bäuerle *et al* [20].

For the compositions $PbZr_{0.86}Ti_{0.14}O_3$ (see figure 3) and $PbZr_{0.88}Ti_{0.12}O_3$ there were observed almost the same qualitative features as were found for $PbZr_{0.90}Ti_{0.10}O_3$—however, with an increase in the rhombohedral (LT) → rhombohedral (HT) → orthorhombic (I) phase

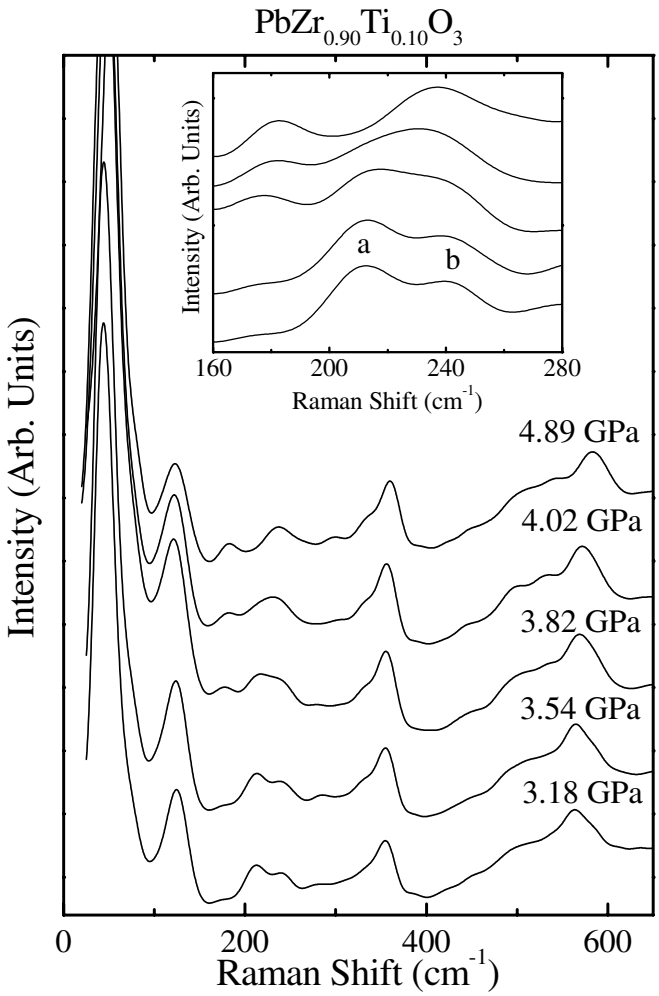

Figure 2. Raman spectra for $PbZr_{0.90}Ti_{0.10}O_3$ ceramics recorded at pressures up to 5.0 GPa. The inset shows a doublet mode behaviour indicating the orthorhombic (I) → orthorhombic (I′) phase transition.

transition pressures and surprisingly a decreasing in the orthorhombic (I) → orthorhombic (I′) transition pressure. Finally, the results for all compositions investigated in this work are summarized in the equilibrium phase diagram (concentration–pressure) for Zr-rich PZT ceramics depicted in figure 4.

The ferroelectricity in perovskite systems has its origin in the subtle balance between long- and short-range interactions [27, 28]. Being a variable that affects this balance strongly, pressure can induce changes in the structure and properties of ferroelectric materials. For the classical ferroelectrics, $PbTiO_3$ and $BaTiO_3$, the pressure induces a phase transition from a ferroelectric phase to a paraelectric cubic phase. $PbZrO_3$ did not present this kind of behaviour. In fact, it was reported that for pressures up to 80 GPa, $PbZrO_3$ did not go to the cubic paraelectric phase [21]. In order to understand these different transitions, we are going to recall theoretical results reported recently [29, 30]. The authors of references [29] and [30] have performed first-principles calculations using local density-functional theory for

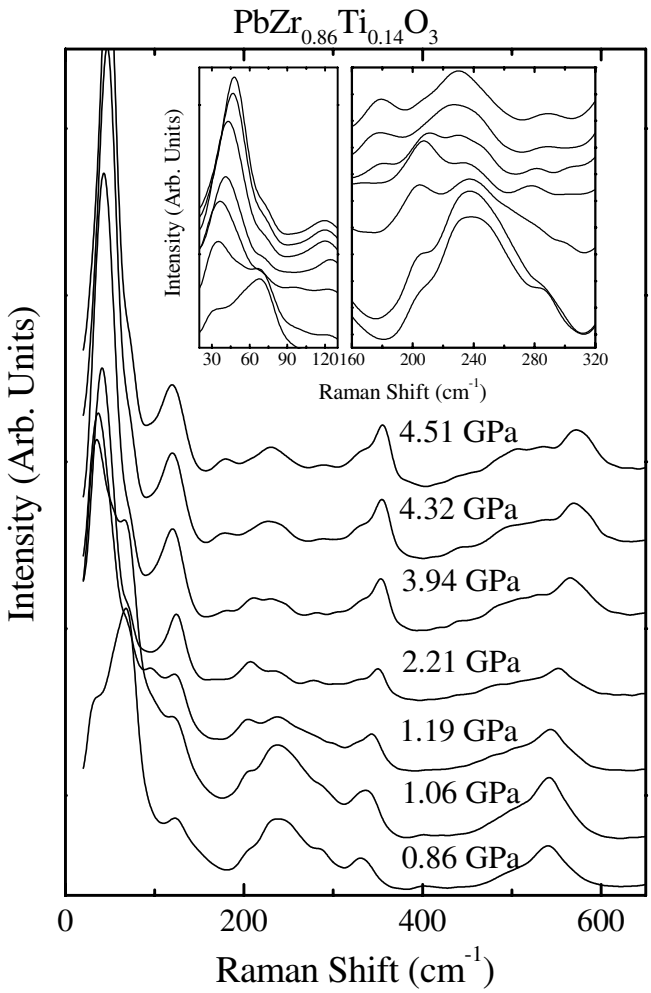

Figure 3. Raman spectra for $PbZr_{0.86}Ti_{0.14}O_3$ ceramics recorded at pressures up to 5.0 GPa. The insets depict the low-frequency region and the doublet mode behaviour.

$PbZrO_3$ in order to unveil the pressure dependence of phonons in perovskite $PbZrO_3$. This analysis is important for understanding the behaviour of PZT under high pressure since the phase transitions in ferroelectric systems are closely related to the freezing in of the zone-centre mode.

$PbZrO_3$ presents modes belonging to six different irreducible representations as follows: R_{25}, R_{15}, $M_{5'}(1/2,1/2,0)$, $X_1(0,0,1/2)$, $\Sigma_3(1/4,1/4,0)$, and $S_3(1/4,1/4,1/2)$. The contributions of each of the modes to the distortion from ideal cubic perovskite structure are very different, and the modes R_{25} and Σ_3 are strongly dominant. It is pointed out that antiferroelectric displacements are associated with Σ_3 modes and R_{25} corresponds to coupled rotations of the corner-connected oxygen octahedra [29]. Also, the very different Zr–O and Ti–O interactions in $PbZrO_3$ suggest a very critical process in the balance between short- and long-range forces. Thus, the ferroelectric-to-antiferroelectric phase transition observed in Zr-rich PZT occurs due to the cooperation and competition among Γ_{TO}, R_{25}, and Σ_3 mode instabilities [29, 30]. The lattice dynamical study made by Ghosez *et al* [29] is limited to the edges of the PZT phase

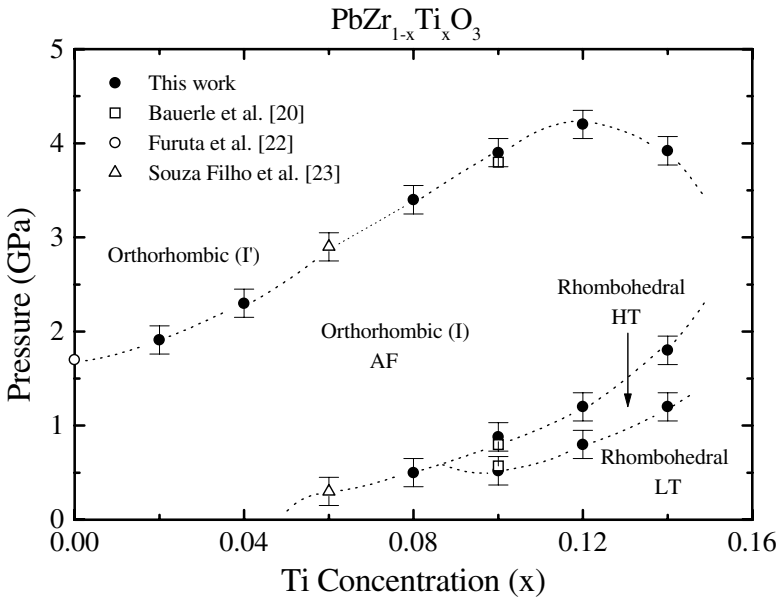

Figure 4. A plot of the concentration–pressure phase diagram for the Zr-rich PZT system. The open squares, open circle, and open triangles are data taken from Bäuerle *et al* [20], Furuta *et al* [22], and Souza Filho *et al* [23], respectively. For all points, the error bar was of the order of 0.15 GPa. The dashed lines are visual guides.

diagram. Application of density-functional theory to PZT is needed in order to complete the description of the phase diagram in a better way. The understanding of mode instabilities in PZT as functions of Zr content and pressure variation should account for the existence of the antiferroelectric phase between two ferroelectric phases. Finally, the complexity of the phase diagram in figure 4 is a challenge for density-functional theory and other theoretical methods such as the weighted-density approximation (WDA). Unfortunately, up to now, a phenomenological study within the framework of Landau–Devonshire theory of these phase transitions has not been possible due to the lack of experimental data on the new high-pressure phases.

4. Conclusions

In conclusion, we have performed a systematic high-pressure Raman study on several $PbZr_{1-x}Ti_xO_3$ samples in order to reveal the effect of the pressure on the stable phases of Zr-rich PZT ceramics. We detected the existence of a triple point among the antiferroelectric orthorhombic (I′), the rhombohedral low-temperature, and the rhombohedral high-temperature phases for a Ti concentration around 0.09. Also, we should point out the possibility of the existence of another triple point in the phase diagram that would result from extension of the antiferroelectric phase. Finally, a possible reason for the richness of the phase diagram for the Zr-rich PZT system is the instability of Γ_{TO}, R_{25}, and Σ_3 modes which is related to the rotation of oxygen octahedra. Since pressure is a 'cleaner' variable for probing short- and long-range interactions, future work with this approach should make it possible to obtain further fundamental information for ferroelectric materials.

Acknowledgments

AGSF acknowledges the fellowship received from Fundação Cearense de Amparo à Pesquisa (FUNCAP). PTCF acknowledges FUNCAP for grant No 017&96 PD. Financial support from CNPq, FAPESP and FINEP, Brazilian funding agencies, is also gratefully acknowledged.

References

[1] Pignolet A, Wang L, Proctor M, Levy F and Schmid P E 1993 *J. Appl. Phys.* **74** 6625
[2] Zhang H, Leppavuori S and Karjalainen P 1995 *J. Appl. Phys.* **77** 2691
[3] Fujishita H and Katano S 1997 *J. Phys. Soc. Japan* **66** 3484
[4] Corker D L, Glazer A M, Whatmore R W, Stallard A and Fauth F 1998 *J. Phys.: Condens. Matter* **10** 6251
[5] Ujma Z, Handerek J, Hassan H, Kugel G E and Pawelczyk M 1995 *J. Phys.: Condens. Matter* **7** 895
[6] Handerek J and Ujma Z 1995 *J. Phys.: Condens. Matter.* **7** 1721
[7] El-Harrad I, Becker P, Carabatos-Nedelec C, Handerek J, Ujma Z and Dimytrov D 1995 *J. Appl. Phys.* **78** 5581
[8] Bäuerle D, Yacoby Y and Ritcher W 1974 *Solid State Commun.* **14** 1137
[9] Agrawal D C, Majumder S B, Mohapatra Y N, Sathaiah S, Bist H D, Katiyar R S, Ching-Prado E and Reynes A 1993 *J. Raman Spectrosc.* **24** 459
[10] Rolender K, Kugel G E, Fontana M D, Handerek J, Lahlon S and Carabatos-Nedelec C 1989 *J. Phys.: Condens. Matter* **1** 2257
[11] Burns G and Scott B A 1970 *Phys. Rev. Lett.* **25** 167
[12] Burns G and Scott B A 1970 *Phys. Rev. Lett.* **25** 1191
[13] Meng J F, Zou G T, Cui Q L, Li J P, Wang X H and Zhao M Y 1994 *J. Phys. Chem. Solids* **55** 427
[14] Meng J F, Katiyar R S, Zou G T and Wang X H 1997 *Phys. Status Solidi* a **164** 851
[15] Jaffe B, Cook W R and Jaffe H 1971 *Piezoelectric Ceramic* (New York: Academic) p 139
[16] Noheda B, Cox D E, Shirane G, Gonzalo J A, Park S-E and Cross L E 1999 *Appl. Phys. Lett.* **74** 2059
[17] Noheda B, Gonzalo J A, Cross L E, Guo R, Park S-E, Moure C, Cox D E and Shirane G 2000 *Phys. Rev.* B **61** 8687
[18] Souza Filho A G, Lima K C V, Ayala A P, Guedes I, Freire P T C, Mendes Filho J, Araújo E B and Eiras J A 2000 *Phys. Rev.* B **61** 14 283
[19] Cerdeira F, Holzapfel W B and Bäuerle J D 1975 *Phys. Rev.* B **11** 1188
[20] Bäuerle D, Holzapfel W B, Pinczuk A and Yacoby Y 1977 *Phys. Status Solidi* a **83** 99
[21] Kobayashi Y, Endo S, Ming L C, Deguchi K, Ashida T and Fujishita H 1999 *J. Phys. Chem. Solids* **60** 57
[22] Furuta H, Endo S, Ming L C and Fujishita H 1999 *J. Phys. Chem. Solids* **60** 65
[23] Souza Filho A G, Freire P T C, Sasaki J M, Guedes I, Mendes Filho J, Melo F E A, Araújo E B and Eiras J A 1999 *Solid State Commun.* **112** 383
[24] Piermarini G J and Block S 1975 *Rev. Sci. Instrum.* **46** 973
[25] Pasto A E and Condrate R E 1993 *J. Am. Ceram. Soc.* **56** 436
[26] Carabatos-Nedelec C, El-Harrad I, Handerek J, Brehat F and Wyncke B 1992 *Ferroelectrics* **125** 483
[27] Samara G A, Sakudo T and Yoshimitsu K 1975 *Phys. Rev. Lett.* **35** 1767
[28] Cohen R E 1992 *Nature* **358** 136
[29] Ghosez Ph, Cockayne E, Waghmare U V and Rabe K M 1999 *Phys. Rev.* B **60** 836
[30] Cockayne E and Rabe K M 2000 *J. Phys. Chem. Solids* **61** 305